Cancer Science
Japanese Cancer Association JCA
Open Access

Antitumor effect of nuclear factor-κB decoy transfer by mannose-modified bubble lipoplex into macrophages in mouse malignant ascites

Yusuke Kono,[1] Shigeru Kawakami,[2] Yuriko Higuchi,[1] Kazuo Maruyama,[3] Fumiyoshi Yamashita[1] and Mitsuru Hashida[1,4]

[1]Department of Drug Delivery Research, Graduate School of Pharmaceutical Sciences, Kyoto University, Kyoto; [2]Division of Analytical Research for Pharmacoinformatics, Graduate School of Biomedical Sciences, Nagasaki University, Nagasaki; [3]Department of Biopharmaceutics, School of Pharmaceutical Science, Teikyo University, Tokyo; [4]Institute for Integrated Cell-Material Sciences, Kyoto University, Kyoto, Japan

Key words

Drug targeting, Ehrlich ascites carcinoma, nuclear factor-κB decoy, sonoporation, tumor-associated macrophages

Correspondence

Shigeru Kawakami, 1-14, Bunkyo-mahci, Nagasaki 606-8501, Japan.
Tel: +81-95-819-2450; Fax: +81-95-819-2450;
E-mail: skawakam@nagasaki-u.ac.jp
and
Mitsuru Hashida, 46-29 Yoshida-shimoadachi-cho, Sakyo-ku, Kyoto 606-8501, Japan.
Tel: +81-75-753-4545; Fax: +81-75-753-4575;
E-mail: hashidam@pharm.kyoto-u.ac.jp

Funding Information

Ministry of Education, Culture, Sports, Science and Technology of Japan; National Institute of Biomedical Innovation; Mochida Memorial Foundation for Medical and Pharmaceutical Research.

Received February 19, 2014; Revised April 28, 2014; Accepted May 16, 2014

Cancer Sci **105** (2014) 1049–1055

doi: 10.1111/cas.12452

Patients with malignant ascites (MAs) display several symptoms, such as dyspnea, nausea, pain, and abdominal tenderness, resulting in a significant reduction in their quality of life. Tumor-associated macrophages (TAMs) play a crucial role in MA progression. Because TAMs have a tumor-promoting M2 phenotype, conversion of the M2 phenotypic function of TAMs would be promising for MA treatment. Nuclear factor-κB (NF-κB) is a master regulator of macrophage polarization. Here, we developed targeted transfer of a NF-κB decoy into TAMs by ultrasound (US)-responsive, mannose-modified liposome/NF-κB decoy complexes (Man-PEG bubble lipoplexes) in a mouse peritoneal dissemination model of Ehrlich ascites carcinoma. In addition, we investigated the effects of NF-κB decoy transfection into TAMs on MA progression and mouse survival rates. Intraperitoneal injection of Man-PEG bubble lipoplexes and US exposure transferred the NF-κB decoy into TAMs effectively. When the NF-κB decoy was delivered into TAMs by this method in the mouse peritoneal dissemination model, mRNA expression of the Th2 cytokine interleukin (IL)-10 in TAMs was decreased significantly. In contrast, mRNA levels of Th1 cytokines (IL-12, tumor necrosis factor-α, and IL-6) were increased significantly. Moreover, the expression level of vascular endothelial growth factor in ascites was suppressed significantly, and peritoneal angiogenesis showed a reduction. Furthermore, NF-κB decoy transfer into TAMs significantly decreased the ascitic volume and number of Ehrlich ascites carcinoma cells in ascites, and prolonged mouse survival. In conclusion, we transferred a NF-κB decoy efficiently by Man-PEG bubble lipoplexes with US exposure into TAMs, which may be a novel approach for MA treatment.

A variety of abdominal tumors, such as ovarian, pancreatic, gastric, and colorectal malignancies, are often accompanied by MAs.[1–4] Patients with MAs display several symptoms, including abdominal pain, respiratory distress, nausea, and anorexia, resulting in a significant reduction of their quality of life.[1–4] In addition, MAs are associated with poor prognoses.[5,6]

Malignant ascites are known to contain an abundance of leukocytes.[7,8] In particular, macrophages are major components of the MA microenvironment, and these TAMs are critically involved in MA progression.[9–11] It has been reported that either depletion or functional regulation of TAMs suppresses the accumulation of ascites and proliferation of cancer cells.[12–14]

Macrophages are generally classified into two phenotypes, M1 and M2, according to their characteristics of humoral factor production and gene expression.[15,16] M1 (classically activated) macrophages have an antitumor potency based on the expression of Th1 cytokines (e.g. IL-12, TNF-α, and IL-6) and nitric oxide production. In contrast, M2 (alternatively activated) macrophages show tumor-promoting effects through expression of several cytokines and pro-tumor factors, such as IL-10, VEGF, and MMPs. Because a large proportion of TAMs are known to show the M2 phenotype,[17–19] phenotypic conversion of TAMs from M2 to M1 would be a promising approach for MA treatment.[20–22]

Recently, it has been reported that inhibition of NF-κB expression and activation can suppress the phenotypic conversion of TAMs to M2.[23–25] We have previously reported that NF-κB inhibition using oligonucleotides, such as siRNA and NF-κB decoy oligonucleotides, show the potential to convert the phenotype of TAMs from M2 toward M1.[26,27] Recently, we have developed US-responsive, mannose-modified liposome /NF-κB decoy complexes (or Man-PEG bubble lipoplexes) for targeting mannose receptors that are highly expressed on the surface of TAMs, and achieved TAM-targeted NF-κB transfection into solid tumors by US exposure in tumor-bearing mice.[27] Based on these findings, we hypothesized that Man-PEG bubble lipoplexes with US exposure in the abdominal area may introduce a NF-κB decoy efficiently into TAMs existing in MAs, resulting in a therapeutic effect.

In the present study, we determined the efficiency of NF-κB decoy transfection by i.p. injection of Man-PEG bubble lipoplexes combined with transdermal US exposure in the abdominal area of EAC-bearing mice. Furthermore, we investigated the effects of NF-κB decoy transfection by this method on the tumor-promoting phenotype of TAMs as well as MA progression.

Materials and Methods

Animals and cell lines. Female ddY mice (4–5 weeks old) were purchased from the Shizuoka Agricultural Cooperative Association for Laboratory Animals (Shizuoka, Japan). All animal experiments were carried out in accordance with the Guide for the Care and Use of Laboratory Animals as adopted and promulgated by the US National Institutes of Health (Bethesda, MD, USA) and the Guidelines for Animal Experiments of Kyoto University (Kyoto, Japan). The protocol was approved by the Kyoto University Animal Experimentation Committee (approval no. 2013-44). All surgery was carried out under sodium pentobarbital anesthesia, and all efforts were made to minimize suffering. The EAC cells were obtained from the Riken Bioresource Center (Osaka, Japan). Cells were cultured in DMEM supplemented with 10% heat-inactivated FBS, penicillin G (100 U/mL), and streptomycin (100 μg/mL) at 37°C in 5% CO_2.

Nuclear factor-κB decoy oligonucleotides. Nuclear factor-κB decoy oligonucleotides, FAM-labeled NF-κB decoy oligonucleotides, and random decoy oligonucleotides were phosphorothioated and kindly provided by AnGes MG (Osaka, Japan). The sequences of the decoy were as follows. Nuclear factor-κB decoy: sense, GGAGGGAAATCCCTTCAAGG and antisense, CCTCCCTTTAGGGAAGTTCC; random decoy: sense, TTGCCGTACCTGACTTAGCC and antisense, AACGGCATG GACTGAATCGG.

Construction of Man-PEG bubble lipoplexes. Man-PEG bubble lipoplexes were constructed according to our previous reports.[27,28] Briefly, to produce the liposomes for bubble lipoplexes, DSDAP, DSPC, and NH_2-PEG-DSPE (Avanti Polar Lipids Inc., Alabaster, AL, USA) or mannose-modified PEGDSPE (Man-PEG-DSPE) were mixed in chloroform at a molar ratio of 7:2:1. The liposome construction mixture was dried by evaporation, vacuum desiccated, and the resultant lipid film was resuspended in a sterile 5% glucose solution. After hydration for 30 min at 65°C, the dispersion was sonicated for 10 min in a bath-type sonicator and then in a tip-type sonicator for 3 min to produce liposomes. The liposomes were sterilized by passing through a 0.45-μm membrane filter (Nihon-Millipore, Tokyo, Japan). Lipoplexes were prepared by gently mixing with equal volumes of NF-κB decoy and liposome solution at a charge ratio of 1.0:2.3 (−:+). To enclose US imaging gas in lipoplexes, perfluoropropane gas (Takachiho Chemical Industries, Tokyo, Japan) was applied to prepare lipoplexes under pressure, which were sonicated using a bath-type sonicator (AS ONE, Osaka, Japan) for 5 min. The particle sizes and ξ-potentials of liposomes/lipoplexes were determined by a Zetasizer Nano ZS instrument (Malvern Instruments, Malvern, UK).

Separation of F4/80$^+$ cells (TAMs) from tumor ascites. Ehrlich ascites carcinoma cells (1×10^6 cells) were inoculated i.p. into mice. The ascites were then harvested at predetermined times post-inoculation. F4/80$^+$ cells were separated by magnetic cell sorting with a phycoerythrin-labeled anti-mouse F4 sol;80 antibody (Bay Bioscience, Hyogo, Japan), phycoerythrin-positive selection kit, and EasySep (Veritas, Tokyo, Japan) following the manufacturer's instructions.

***In vivo* internalization study.** At 4 days post-i.p. inoculation of EAC cells into mice, 200 μL of bubble lipoplexes constructed with the FAM-labeled NF-κB decoy (10 μg NF-κB decoy) was injected i.p. At 5 min post-injection, US (frequency, 1.056 MHz; duty, 50%; burst rate, 10 Hz; intensity, 1.0 W/cm^2; time, 2 min) was exposed transdermally to the abdominal area using a Sonopore-4000 sonicator (NEPA GENE, Chiba, Japan) with a probe of 20 mm in diameter. At 1 h post-injection, the ascites were harvested to separate the TAMs. The cell-associated fluorescence in 10 000 cells was measured using a BD FACSCanto II Flow Cytometer (Becton Dickinson, Tokyo, Japan).

***In vivo* NF-κB decoy transfection.** The EAC-bearing mice were i.p. injected with 200 μL Bare-PEG or Man-PEG bubble lipoplexes (10 μg NF-κB decoy). At 5 min post-injection, US (frequency, 1.056 MHz; duty, 50%; burst rate, 10 Hz; intensity, 1.0 W/cm^2; time, 2 min) was exposed transdermally to the abdominal area using the Sonopore-4000 sonicator and 20-mm-diameter probe.

Measurement of intranuclear NF-κB. At 4 days after inoculation of EAC cells into mice, we carried out *in vivo* NF-κB decoy transfection. After 12 h of *in vivo* NF-κB decoy transfection, the ascites were harvested, and TAMs were separated from ascites. Nuclear extracts of the TAMs were prepared using a Nuclear Extract Kit (Active Motif, Carlsbad, CA, USA). Nuclear proteins were stored at −80°C until use. The protein concentration was measured with a Protein Quantification Kit (Dojindo Molecular Technologies, Tokyo, Japan). The amounts of p50 and p65, which are the components of NF-κB, in the nuclear extracts were measured using a TransAM NFκB Family Kit (Active Motif) according to the recommended procedures.

Quantitative RT-PCR. At 4 days after inoculation of EAC cells into mice, we carried out *in vivo* NF-κB decoy transfection. After 24 h of *in vivo* NF-κB decoy transfection, the ascites were harvested, and TAMs were separated from ascites. Total RNA was isolated from TAMs using a GenElute Mammalian Total RNA Miniprep Kit (Sigma-Aldrich, St. Louis, MO, USA). Reverse transcription of mRNA was carried out using a PrimeScript RT reagent Kit (Takara Bio, Shiga, Japan). Detection of cDNAs (IL-10, IL-12p70, TNF-α, IL-6, VEGF-A, and GAPDH) was carried out by real-time PCR using SYBR Premix Ex Taq (Takara Bio) and a LightCycler Quick System 350S (Roche Diagnostics, Indianapolis, IN, USA). The primers for IL-10, IL-12, TNF-α, IL-6, and GAPDH cDNAs were as follows: IL-10, 5′-GCT CTT ACT GAC TGG CAT GAG-3′ (forward) and 5′-CGC AGC TCT AGG AGC ATG TG-3′ (reverse); IL-12, 5′-ACT CTG CGC CAG AAA CCT C-3′ (forward) and 5′-CAC CCT GTT GAT GGT CAC GAC-3′ (reverse); TNF-α, 5′-CCT CCC TCT CAT CAG TTC TA-3′ (forward) and 5′-ACT TGG TGG TTT GCT ACG AC-3′ (reverse); IL-6, 5′-TAG TCC TTC CTA CCC CAA TTT CC -3′ (forward) and 5′-TTG GTC CTT AGC CAC TCC TTC-3′ (reverse); VEGF-A, 5′- AGC ACA GCA GAT GTG AAT GC-3′ (forward) and 5′-AAT GCT TTC TCC GCT CTG AA-3′ (reverse); and GAPDH, 5′-TCT CCT GCG ACT TCA ACA-3′ (forward) and 5′-GCT GTA GCC GTA TTC ATT GT-3′ (reverse).

Measurement of VEGF concentrations in ascites. At 2 days after inoculation of EAC cells into mice, *in vivo* NF-κB decoy transfection was carried out three times every other day (days 2, 4, and 6 after inoculation of EAC cells). Ascites were har-

vested at 10 days after EAC cell inoculation. The ascites were centrifuged at 10 000 *g* for 10 min at 4°C and the resultant supernatant was applied to a commercial ELISA kit (PeproTech, Rocky Hill, NJ, USA) to measure the concentration of VEGF.

Determination of angiogenesis. At 2 days after inoculation of EAC cells, *in vivo* NF-κB decoy transfection was carried out three times every other day (days 2, 4, and 6 after inoculation of EAC cells). At 10 days after EAC cell inoculation, the mice were photographed, their peritoneum was cut open, and then the inner lining of the peritoneal cavity was photographed.

Measurement of ascitic fluid. At 2 days after inoculation of EAC cells, *in vivo* NF-κB decoy transfection was carried out three times every other day (days 2, 4, and 6 after inoculation of EAC cells). At 10 days after EAC cell inoculation, the volume of the ascitic fluid was determined by aspiration with a needle and syringe.

Measurement of the number of EAC cells in ascites. To measure EAC cell numbers, EAC cells with stable expression of the firefly luciferase gene (EAC/Luc) were established as reported previously.[29] At 2 days after inoculation of EAC/Luc cells into mice, *in vivo* NF-κB decoy transfection was carried out three times every other day (days 2, 4, and 6 after inoculation of EAC cells). After 10 days of EAC/Luc cell inoculation, 500 μL ascites was harvested and mixed with an equal volume of lysis buffer (0.05% Triton X-100, 2 mM EDTA, and 0.1 M Tris, pH 7.8). Then the mixed solution was centrifuged at 10 000 *g* for 10 min at 4°C. The supernatant was mixed with luciferase assay buffer (Picagene; Toyo Ink, Tokyo, Japan) and the luciferase activity was measured in a luminometer (Lumat LB 9507; EG&G Berthold, Bad Wildbad, Germany). The luciferase activity in the ascites was converted to the number of EAC/Luc cells using a regression line.

Measurement of the body weight and survival rates of EAC-bearing mice. The body weight of EAC-bearing mice was measured every day until the death of the first mice. The survival of mice was monitored up to 60 days after EAC cell inoculation.

Statistical analysis. Results are presented as the mean ± SD of more than three experiments; ANOVA was used to test the statistical significance of differences among groups. Two-group comparisons were carried out using Student's *t*-test. Multiple comparisons between control groups and other groups were carried out by Dunnett's test, and multiple comparisons between all groups used the Tukey–Kramer test. Survival curves were compared using the log–rank test.

Results

Physicochemical properties of bubble lipoplexes. The physicochemical properties of bubble lipoplexes were evaluated by measuring the particle sizes and ζ-potentials. Mean particle sizes and ζ-potentials of Bare-PEG and Man-PEG bubble lipoplexes were approximately 550 nm and +20 mV, respectively (Table 1). These results are comparable with our previous report.[27]

***In vivo* NF-κB decoy transfer into TAMs.** We carried out *in vivo* TAM-targeted NF-κB decoy transfer by Man-PEG bubble lipoplexes constructed with a FAM-labeled NF-κB decoy combined with US exposure. The amount of FAM-labeled NF-κB decoy introduced into TAMs by Man-PEG bubble lipoplexes and US exposure was eightfold higher than that by Man-PEG bubble lipoplexes without US exposure (Fig. 1). Moreover, this level of FAM-labeled NF-κB decoy transfection by Man-PEG bubble lipoplexes and US exposure was much higher than that by Bare-PEG bubble lipoplexes and US exposure. Similarly, intranuclear p50 and p65 levels in TAMs were significantly decreased by NF-κB decoy transfer using Man-PEG bubble lipoplexes and US exposure (Fig. 2).

Table 1. Particle sizes and ζ-potentials of liposomes and lipoplexes

	Particle size, nm	ζ-Potential, mV
Bare-PEG bubble liposome (DSDAP:DSPC: NH_2-PEG_{2000}-DSPE = 7:2:1 [mol])	561.1 ± 6.3	34.4 ± 1.4
Man-PEG bubble liposome (DSDAP:DSPC: Man-PEG_{2000}-DSPE = 7:2:1 [mol])	556.2 ± 3.9	35.8 ± 0.7
Bare-PEG bubble lipoplex (DSDAP:DSPC: NH_2-PEG_{2000}-DSPE = 7:2:1 [mol])	550.8 ± 5.7	19.9 ± 2.2
Man-PEG bubble lipoplex (DSDAP:DSPC: Man-PEG_{2000}-DSPE = 7:2:1 [mol])	557.6 ± 4.9	19.6 ± 3.1

Bare-PEG bubble liposome, ultrasound (US)-responsive and mannose-unmodified liposome; DSDAP, 1,2-distearoyl-sn-glycero-3-dimethylammonium propane, 1,2-distearoyl-sn-glycero-3-phosphocholine; DSPC, 1,2-distearoyl-sn-glycero-3-phosphocholine; DSPE, 1,2-distearoyl-sn-glycero-3-phosphoethanolamine; Man-PEG bubble liposome, US-responsive and mannose-modified liposome; Bare-PEG bubble lipoplex, US-responsive and mannose-unmodified liposome/nuclear factor (NF)-κB decoy complexes; Man-PEG bubble lipoplex, US-responsive and mannose-modified liposome/NF-κB decoy complexes.

Change of cytokine mRNA expression in TAMs. Because the phenotype of macrophages is generally classified according to the profile of cytokine expression,[15,16] we assessed the expression levels of cytokine mRNA in TAMs transfected with the NF-κB decoy. Expression of IL-10 mRNA in TAMs transfected with the NF-κB decoy by Man-PEG bubble lipoplexes and US exposure was the lowest among all groups (Fig. 3a). In contrast, mRNA expression levels of IL-12, TNF-α, and IL-6 in TAMs transfected with the NF-κB decoy by Man-PEG bubble lipoplexes and US exposure were significantly higher compared with those in other groups (Fig. 3b–d).

Suppressive effect of NF-κB decoy transfection on tumor angiogenesis. Angiogenesis is a critical event for the progression of MA.[30–32] Because VEGF predominantly regulates angiogenesis,[33,34] the level of VEGF in tumor ascites and the expression levels of VEGF mRNA in TAMs were determined after NF-κB decoy transfection into TAMs. As shown in Figure 4(a), the concentration of VEGF in the ascites was significantly low in mice transfected with the NF-κB decoy by Man-PEG bubble lipoplexes and US exposure. In addition, expression of VEGF mRNA in TAMs transfected with the NF-κB decoy by Man-PEG bubble lipoplexes and US exposure was the lowest among all groups (Fig. 4b). Moreover, we evaluated the degree of angiogenesis in the peritoneum after NF-κB decoy transfection into TAMs. As shown in Figure 4(c), suppressed angiogenesis in the peritoneum was observed in mice transfected with the NF-κB decoy by Man-PEG bubble lipoplexes and US exposure.

Antitumor effects of NF-κB decoy transfection into TAMs on EAC-bearing mice. Finally, we examined the antitumor effects of NF-κB decoy transfection into TAMs using Man-PEG bubble lipoplexes and US exposure against MA. The strongest inhibitory effect on EAC cell proliferation in ascites and ascitic fluid increase was observed by NF-κB decoy transfection into TAMs using Man-PEG bubble lipoplexes and US exposure (Fig. 5a,b). In addition, the increase of body weight was significantly suppressed and the survival of EAC-bearing mice was significantly prolonged by NF-κB decoy transfection into

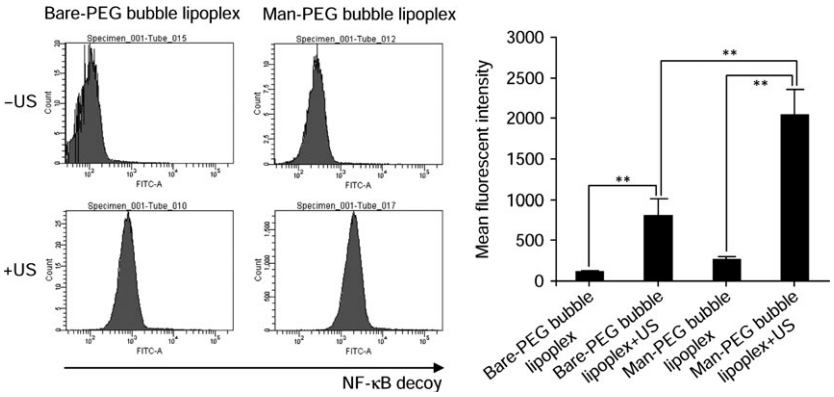

Fig. 1. *In vivo* transfection efficiency of the nuclear factor-κB (NF-κB) decoy into tumor-associated macrophages by ultrasound (US)-responsive and mannose-unmodified liposome/NF-κB decoy complexes (Bare-PEG bubble lipoplexes) and ultrasound (US)-responsive and mannose-modified liposome /NF-κB decoy complexes (Man-PEG bubble lipoplexes) (10 μg NF-κB decoy) with (+) or without (–) US exposure. Fluorescent intensity of the FAM-labeled NF-κB decoy in tumor-associated macrophages at 1 h after addition of bubble lipoplexes. $^{**}P < 0.01$.

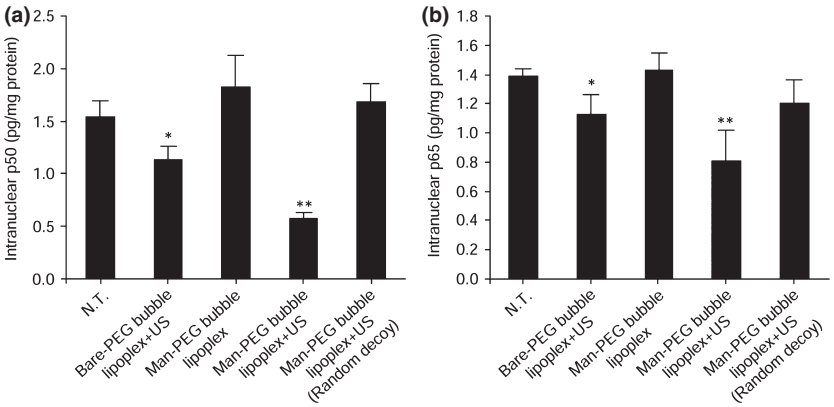

Fig. 2. Amounts of intranuclear p50 (a) and p65 (b) in tumor-associated macrophages following *in vivo* nuclear factor-κB (NF-κB) decoy transfection using ultrasound (US)-responsive and mannose-unmodified liposome/NF-κB decoy complexes (Bare-PEG bubble lipoplexes) or ultrasound (US)-responsive and mannose-modified liposome/NF-κB decoy complexes (Man-PEG bubble lipoplexes) (10 μg NF-κB decoy) with or without US exposure at 12 h post-transfection. Each value represents the mean + SD ($n = 3$). $^{*}P < 0.05$, $^{**}P < 0.01$ compared with non-treatment (N.T.).

TAMs using Man-PEG bubble lipoplexes and US exposure (Fig. 5c,d).

Discussion

In this study, we applied the combined use of Man-PEG bubble lipoplexes and US exposure for TAM-targeted delivery of a NF-κB decoy in EAC-bearing mice. Man-PEG bubble lipoplexes possess the following two hallmarks: (i) mannose receptor-mediated cell-selective targeting; and (ii) direct delivery of nucleic acids into the cytoplasm by "sonoporation."[28,35–37] Because TAMs are known to express high levels of mannose receptor on their surface,[9,38] we hypothesized that Man-PEG bubble lipoplexes would achieve efficient delivery of a NF-κB decoy into TAMs in EAC-bearing mice. We showed that the combined use of Man-PEG bubble lipoplexes with US exposure was able to introduce the NF-κB decoy into TAMs compared with using Bare-PEG bubble lipoplexes and US exposure or Man-PEG bubble lipoplexes without US exposure (Fig. 1). As we previously showed that a large proportion of Man-PEG bubble lipoplexes was bound to the surface of macrophages, not internalized by endocytosis, at 5 min after the addition of Man-PEG bubble lipoplexes,[39] we assumed that NF-κB decoy would be introduced into the cytoplasm of TAMs directly by the collapse of Man-PEG bubble lipoplexes on the surface of TAMs following US exposure.

It is assumed that the mechanism of the phenotypic conversion of TAMs is related to a reduction of intranuclear p50 in TAMs. Nuclear factor-κB is composed of p50 and p65;[40–42] p65 possesses a transactivation domain, but p50 does not. Therefore, the NF-κB heterodimer p65/p50 can activate the transcriptional process, which is essential for Th1 immune responses. In contrast, p50/p50 homodimers inhibit transcriptional activation.[40–43] Saccani *et al.* and Porta *et al.* have reported that abundant nucleic accumulation of the p50 NF-κB subunit in TAMs inhibits M1 polarization, and ablation of the p50 subunit prevents TAM polarization to the M2 phenotype.[24,25] The NF-κB decoy used in this study disrupted NF-κB activity by binding to NF-κB p50, and we showed a reduction of nucleic p50 in TAMs after NF-κB decoy transfection (Fig. 2a). These results suggest that phenotypic conversion of TAMs is induced by efficient NF-κB decoy transfection into TAMs.

We determined the changes of both Th1 and Th2 cytokine expression in TAMs with or without NF-κB decoy transfection. As shown in Figure 3(a), mRNA expression of the Th2 cytokine IL-10 in TAMs transfected with the NF-κB decoy by Man-PEG bubble lipoplexes and US exposure was significantly lower compared with that in other groups. In contrast, mRNA levels of Th1 cytokines IL-12, TNF-α, and IL-6 in TAMs transfected with the NF-κB decoy by Man-PEG bubble lipoplexes and US exposure were the highest (Fig. 3b–d). These alterations of cytokine expression levels are in line with our previous report that showed the conversion of cytokine production profiles in TAMs by NF-κB decoy transfection into solid tumor (colon26)-bearing mice.[27] In addition, NF-κB decoy transfection by Man-PEG bubble lipoplexes and US exposure did not affect the viability of TAMs (data not shown). These results suggest that TAMs transfected with a NF-κB decoy by Man-PEG bubble lipoplexes and US exposure convert their phenotype from M2 toward M1.

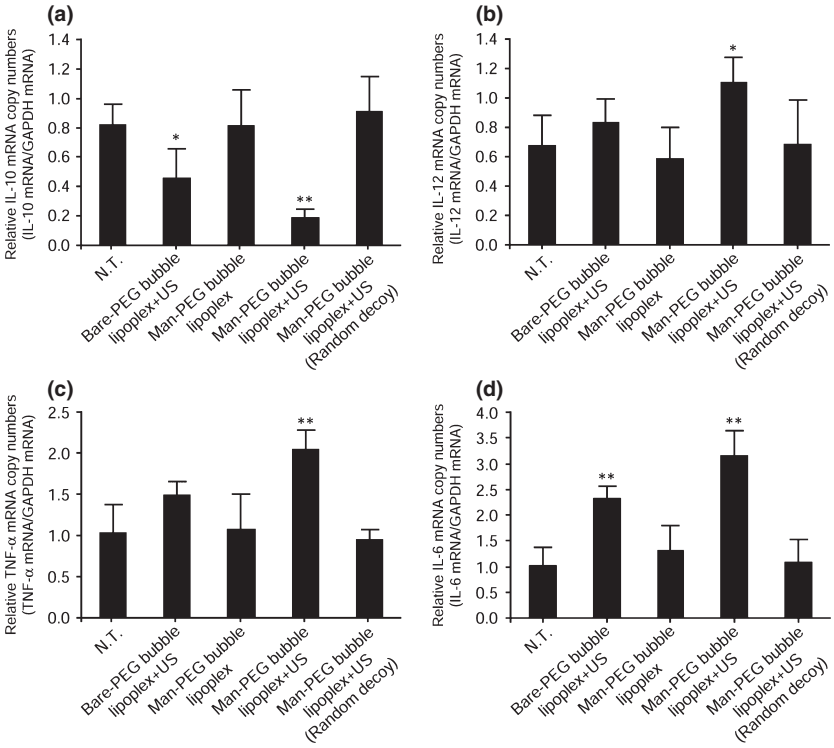

Fig. 3. Effect of *in vivo* nuclear factor-κB (NF-κB) decoy transfection by ultrasound (US)-responsive and mannose-unmodified liposome/NF-κB decoy complexes (Bare-PEG bubble lipoplexes) or ultrasound (US)-responsive and mannose-modified liposome/NF-κB decoy complexes (Man-PEG bubble lipoplexes) (10 μg NF-κB decoy) with or without US exposure on cytokine mRNA expression in tumor-associated macrophages. mRNA levels of interleukin-10 (IL-10) (a), IL-12 (b), tumor necrosis factor-α (TNF-α) (c), and IL-6 (d) in tumor-associated macrophages collected at 24 h post-transfection. Data are represented as the mean + SD ($n = 4$). $^{*}P < 0.05$, $^{**}P < 0.01$ compared with non-treatment (N.T.).

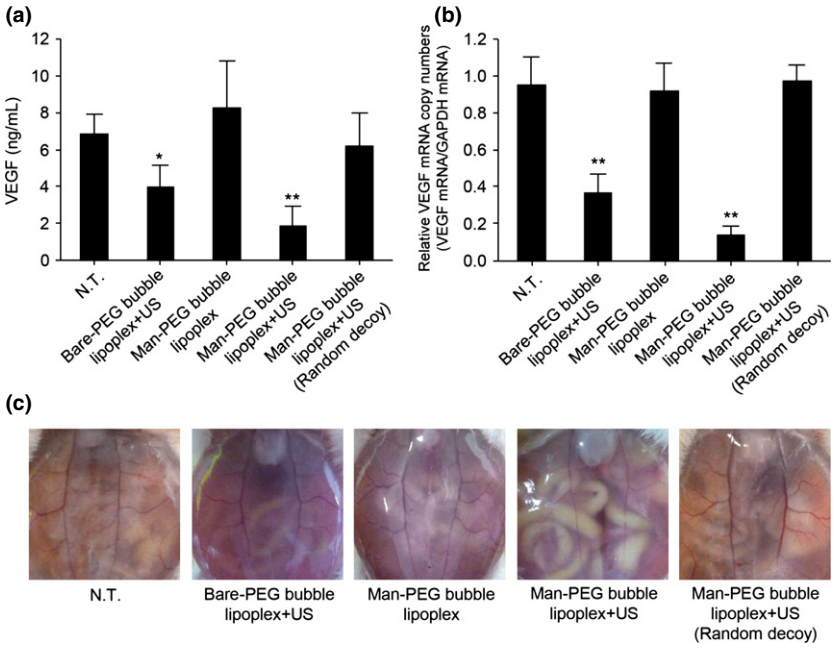

Fig. 4. Effect of *in vivo* nuclear factor-κB (NF-κB) decoy transfection by ultrasound (US)-responsive and mannose-unmodified liposome/NF-κB decoy complexes (Bare-PEG bubble lipoplexes) or ultrasound (US)-responsive and mannose-modified liposome/NF-κB decoy complexes (Man-PEG bubble lipoplexes) (10 μg NF-κB decoy) with or without US exposure on tumor angiogenesis. (a) Vascular endothelial growth factor (VEGF) concentration in ascites collected 10 days after Ehrlich ascites carcinoma cell inoculation into mice. (b) mRNA levels of VEGF in tumor-associated macrophages collected 24 h post-transfection. Data are represented as the mean + SD ($n = 4$). $^{*}P < 0.05$, $^{**}P < 0.01$ compared with non-treatment (N.T.). (c) Peritoneal angiogenesis at 10 days after Ehrlich ascites carcinoma cell inoculation into mice. The peritoneum was cut open and the inner lining of the peritoneal cavity was photographed.

To investigate the therapeutic potential of NF-κB decoy transfer by mannose-modified bubble lipoplexes into TAMs against EAC-bearing mice, we measured ascitic volumes and the number of EAC cells in ascites, and monitored body weight changes and survival of EAC-bearing mice. Saccani *et al.*[24] have reported that TAMs cultured in standard conditions for 24-72 h showed altered characteristics, such as cytokine expression. Taking this into consideration, we designed a protocol in which EAC-bearing mice were i.p. injected with NF-κB decoys three times every other day. As shown in Figure 5(a,b), the strongest inhibitory effects on ascites and EAC cell accumulation in the peritoneal cavity were observed in mice with NF-κB decoy transfer by Man-PEG bubble lipoplexes and US exposure. As we have confirmed that NF-κB decoy transfer had no direct cytotoxic effect on EAC cells (Fig. S1), this therapeutic effect may be attributed to the regulation of TAM function. Furthermore, we observed a significant prolongation of survival and suppression of the increase of body weight (Fig. 5c,d). Taken together, our results indicate that NF-κB decoy transfer by Man-PEG bubble lipoplexes and US exposure into TAMs is an effective method to inhibit MA progression in a mouse peritoneal dissemination model of EAC.

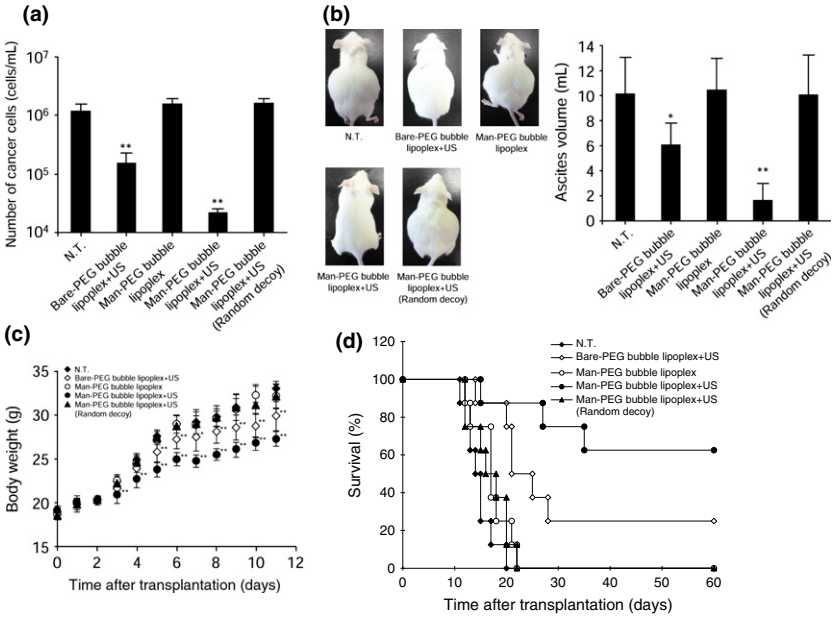

Fig. 5. Effect of *in vivo* nuclear factor-κB (NF-κB) decoy transfection by ultrasound (US)-responsive and mannose-unmodified liposome/NF-κB decoy complexes (Bare-PEG bubble lipoplexes) or ultrasound (US)-responsive and mannose-modified liposome/NF-κB decoy complexes (Man-PEG bubble lipoplexes) (10 μg NF-κB decoy) with or without US exposure on tumor growth and mouse survival. The number of Ehrlich ascites carcinoma (EAC) cells in ascites (a) and the volume of ascites (b) 10 days after EAC cell inoculation into mice. Data are represented as the mean + SD ($n = 4$). $^*P < 0.05$, $^{**}P < 0.01$ compared with non-treatment (N.T.). The body weight (c) and survival (d) of EAC-bearing mice post-transfection. Data are represented as the mean ± SD ($n = 8$). Survival was monitored up to 60 days after EAC cell inoculation into mice. $^*P < 0.05$, $^{**}P < 0.01$ compared with N.T.

Angiogenesis is strongly linked to tumor growth and metastasis.[30–32] It is also known that ascitic tumor growth including EAC is dependent on angiogenesis, and inhibition of angiogenesis exerts a significant antitumor effect in EAC-bearing mice.[30,31,44,45] Because TAMs are reported to promote tumor angiogenesis through expression of VEGF,[17–19] phenotypic regulation of TAMs is expected to suppress angiogenesis in EAC-bearing mice. As shown in Figure 4, VEGF expression in ascites and in TAMs were significantly reduced and peritoneal angiogenesis was more suppressed in the mouse peritoneal dissemination model of EAC transfected with the NF-κB decoy by Man-PEG bubble lipoplexes and US exposure. In addition, we have observed that NF-κB decoy transfer had no direct cytotoxic effect on vascular endothelial cells (normal HUVECs) (Fig. S1). Taking these factors into consideration, suppression of angiogenesis by NF-κB decoy transfer into TAMs might be supported by phenotypic conversion of TAMs and their antitumor effect in the mouse peritoneal dissemination model of EAC.

In conclusion, we succeeded in efficiently delivering a NF-κB decoy into TAMs by Man-PEG bubble lipoplexes and US exposure in a mouse peritoneal dissemination model of EAC. Moreover, we observed potent antitumor effects against MA by efficient transfer of the NF-κB decoy into TAMs. Although further studies are needed to clarify the mechanism, efficient NF-κB decoy transfer by Man-PEG bubble lipoplexes with US exposure into TAMs may be a novel approach for MA treatment.

Acknowledgments

This work was supported in part by a Grant-in-Aid for Scientific Research on Innovative Areas and Young Scientists (A) from the Ministry of Education, Culture, Sports, Science and Technology of Japan, the Programs for Promotion of Fundamental Studies in Health Sciences of the National Institute of Biomedical Innovation, and the Mochida Memorial Foundation for Medical and Pharmaceutical Research.

Disclosure Statement

The authors have no conflict of interest.

Abbreviations

Bare-PEG	mannose-unmodified NH_2-PEG-DSPE
DSPE	1,2-distearoyl-sn-glycero-3-phosphoethanolamine
EAC	hrlich ascites carcinoma
FAM	6-carboxyfluorescein
IL	interleukin
MA	malignant ascite
Man-PEG bubble lipoplexes	ultrasound-responsive and mannose-modified liposome/nuclear factor-κB decoy complexes
NF-κB	nuclear factor-κB
PEG	polyethylene glycol-2000
TAM	tumor-associated macrophage
TNF-α	tumor necrosis factor-α
US	ultrasound
VEGF	vascular endothelial growth factor

References

1 Cavazzoni E, Bugiantella W, Graziosi L, Franceschini MS, Donini A. Malignant ascites: pathophysiology and treatment. *Int J Clin Oncol* 2013; **18**: 1–9.
2 Becker G, Galandi D, Blum HE. Malignant ascites: systematic review and guideline for treatment. *Eur J Cancer* 2006; **42**: 589–97.
3 Ahmed N, Stenvers KL. Getting to know ovarian cancer ascites: opportunities for targeted therapy-based translational research. *Front Oncol* 2013; **3**: 256.
4 Saif MW, Siddiqui IA, Sohail MA. Management of ascites due to gastrointestinal malignancy. *Ann Saudi Med* 2009; **29**: 369–77.
5 Ayantunde AA, Parsons SL. Pattern and prognostic factors in patients with malignant ascites: a retrospective study. *Ann Oncol* 2007; **18**: 945–9.
6 Sangisetty SL, Miner TJ. Malignant ascites: a review of prognostic factors, pathophysiology and therapeutic measures. *World J Gastrointest Surg* 2012; **4**: 87–95.
7 Wang X, Deavers M, Patenia R *et al.* Monocyte/macrophage and T-cell infiltrates in peritoneum of patients with ovarian cancer or benign pelvic disease. *J Transl Med* 2006; **4**: 30.
8 Peter S, Bak G, Hart K, Berwin B. Ovarian tumor-induced T cell suppression is alleviated by vascular leukocyte depletion. *Transl Oncol* 2009; **2**: 291–9.
9 Hagemann T, Wilson J, Burke F *et al.* Ovarian cancer cells polarize macrophages toward a tumor-associated phenotype. *J Immunol* 2006; **176**: 5023–32.
10 Robinson-Smith TM, Isaacsohn I, Mercer CA *et al.* Macrophages mediate inflammation-enhanced metastasis of ovarian tumors in mice. *Cancer Res* 2007; **67**: 5708–16.

11 Takahashi K, Komohara Y, Tashiro H *et al.* Involvement of M2-polarized macrophages in the ascites from advanced epithelial ovarian carcinoma in tumor progression via Stat3 activation. *Cancer Sci* 2010; **101**: 2128–36.
12 Majumder B, Biswas R, Chattopadhyay U. Prolactin regulates antitumor immune response through induction of tumoricidal macrophages and release of IL-12. *Int J Cancer* 2002; **97**: 493–500.
13 Duluc D, Delneste Y, Tan F *et al.* Tumor-associated leukemia inhibitory factor and IL-6 skew monocyte differentiation into tumor-associated macrophage-like cells. *Blood* 2007; **110**: 4319–30.
14 Bak SP, Walters JJ, Takeya M, Conejo-Garcia JR, Berwin BL. Scavenger receptor-A-targeted depletion inhibits peritoneal ovarian tumor progression. *Cancer Res* 2007; **67**: 4783–9.
15 Mosser DM. The many faces of macrophage activation. *J Leukoc Biol* 2003; **73**: 209–12.
16 Sica A, Mantovani A. Macrophage plasticity and polarization: in vivo veritas. *J Clin Invest* 2012; **122**: 787–95.
17 Mantovani A, Sozzani S, Locati M, Allavena P, Sica A. Macrophage polarization: tumor-associated macrophages as a paradigm for polarized M2 mononuclear phagocytes. *Trends Immunol* 2002; **23**: 549–55.
18 Siveen KS, Kuttan G. Role of macrophages in tumour progression. *Immunol Lett* 2009; **123**: 97–102.
19 Biswas SK, Allavena P, Mantovani A. Tumor-associated macrophages: functional diversity, clinical significance, and open questions. *Semin Immunopathol* 2013; **35**: 585–600.
20 Watkins SK, Egilmez NK, Suttles J, Stout RD. IL-12 rapidly alters the functional profile of tumor-associated and tumor-infiltrating macrophages in vitro and in vivo. *J Immunol* 2007; **178**: 1357–62.
21 Na YR, Yoon YN, Son DI, Seok SH. Cyclooxygenase-2 inhibition blocks M2 macrophage differentiation and suppresses metastasis in murine breast cancer model. *PLoS One* 2013; **8**: e63451.
22 Zhang X, Tian W, Cai X *et al.* Hydrazinocurcumin encapsulated nanoparticles "re-educate" tumor-associated macrophages and exhibit anti-tumor effects on breast cancer following STAT3 suppression. *PLoS One* 2013; **8**: e65896.
23 Hagemann T, Lawrence T, McNeish I *et al.* "Re-educating" tumor-associated macrophages by targeting NF-κB. *J Exp Med* 2008; **205**: 1261–8.
24 Saccani A, Schioppa T, Porta C *et al.* p50 nuclear factor-κB overexpression in tumor-associated macrophages inhibits M1 inflammatory responses and antitumor resistance. *Cancer Res* 2006; **66**: 11432–40.
25 Porta C, Rimoldi M, Raes G *et al.* Tolerance and M2 (alternative) macrophage polarization are related processes orchestrated by p50 nuclear factor κB. *Proc Natl Acad Sci U S A* 2009; **106**: 14978–83.
26 Kono Y, Kawakami S, Higuchi Y, Yamashita F, Hashida M. In vitro evaluation of inhibitory effect of nuclear factor-kappa B activity by small interfering RNA on pro-tumor characteristics of M2-like macrophages. *Biol Pharm Bull* 2014; **37**: 137–44.
27 Kono Y, Kawakami S, Higuchi Y, Maruyama K, Yamashita F, Hashida M. Tumour-associated macrophages targeted transfection with NF-κB decoy /mannose-modified bubble lipoplexes inhibits tumour growth in tumour-bearing mice. *J Drug Target* 2014; **22**: 439–49.
28 Un K, Kawakami S, Suzuki R, Maruyama K, Yamashita F, Hashida M. Development of ultrasound-responsive and mannose-modified gene carrier for DNA vaccine therapy. *Biomaterials* 2010; **31**: 7813–26.
29 Hyoudou K, Nishikawa M, Umeyama Y, Kobayashi Y, Yamashita F, Hashida M. Inhibition of metastatic tumor growth in mouse lung by repeated administration of polyethylene glycol-conjugated catalase: quantitative analysis with firefly luciferase-expressing melanoma cells. *Clin Cancer Res* 2004; **10**: 7685–91.
30 Kobold S, Hegewisch-Becker S, Oechsle K, Jordan K, Bokemeyer C, Atanackovic D. Intraperitoneal VEGF inhibition using bevacizumab: a potential approach for the symptomatic treatment of malignant ascites? *Oncologist* 2009; **14**: 1242–51.
31 Agrawal SS, Saraswati S, Mathur R, Pandey M. Cytotoxic and antitumor effects of brucine on Ehrlich ascites tumor and human cancer cell line. *Life Sci* 2011; **89**: 147–58.
32 Masoumi Moghaddam S, Amini A, Morris DL, Pourgholami MH. Significance of vascular endothelial growth factor in growth and peritoneal dissemination of ovarian cancer. *Cancer Metastasis Rev* 2012; **31**: 143–62.
33 Shibuya M. Vascular endothelial growth factor and its receptor system: physiological functions in angiogenesis and pathological roles in various diseases. *J Biochem* 2013; **153**: 13–9.
34 Claesson-Welsh L, Welsh M. VEGFA and tumour angiogenesis. *J Intern Med* 2013; **273**: 114–27.
35 Un K, Kawakami S, Higuchi Y *et al.* Involvement of activated transcriptional process in efficient gene transfection using unmodified and mannose-modified bubble lipoplexes with ultrasound exposure. *J Control Release* 2011; **156**: 355–63.
36 Un K, Kawakami S, Suzuki R, Maruyama K, Yamashita F, Hashida M. Suppression of melanoma growth and metastasis by DNA vaccination using an ultrasound-responsive and mannose-modified gene carrier. *Mol Pharm* 2011; **8**: 543–54.
37 Un K, Kawakami S, Yoshida M *et al.* Efficient suppression of murine intracellular adhesion molecule-1 using ultrasound-responsive and mannose-modified lipoplexes inhibits acute hepatic inflammation. *Hepatology* 2012; **56**: 259–69.
38 Allavena P, Chieppa M, Bianchi G *et al.* Engagement of the mannose receptor by tumoral mucins activates an immune suppressive phenotype in human tumor-associated macrophages. *Clin Dev Immunol* 2010; **2010**: 547179.
39 Un K, Kawakami S, Yoshida M *et al.* The elucidation of gene transferring mechanism by ultrasound-responsive unmodified and mannose-modified lipoplexes. *Biomaterials* 2011; **32**: 4659–69.
40 Gilmore TD. Introduction to NF-κB: players, pathways, perspectives. *Oncogene* 2006; **25**: 6680–4.
41 Mancino A, Lawrence T. Nuclear factor-κB and tumor-associated macrophages. *Clin Cancer Res* 2010; **16**: 784–9.
42 Biswas SK, Lewis CE. NF-κB as a central regulator of macrophage function in tumors. *J Leukoc Biol* 2010; **88**: 877–84.
43 Driessler F, Venstrom K, Sabat R, Asadullah K, Schottelius AJ. Molecular mechanisms of interleukin-10-mediated inhibition of NF-κB activity: a role for p50. *Clin Exp Immunol* 2004; **135**: 64–73.
44 El-Azab M, Hishe H, Moustafa Y. El-Awady el-S. Anti-angiogenic effect of resveratrol or curcumin in Ehrlich ascites carcinoma-bearing mice. *Eur J Pharmacol* 2011; **652**: 7–14.
45 Saraswati S, Alhaider AA, Agrawal SS. Punarnavine, an alkaloid from Boerhaavia diffusa exhibits anti-angiogenic activity via downregulation of VEGF in vitro and in vivo. *Chem Biol Interact* 2013; **206**: 204–13.

Supporting Information

Additional supporting information may be found in the online version of this article:

Fig. S1. Effect of *in vitro* NF-κB decoy transfection by Man-PEG bubble lipoplexes with US exposure on cell viability.

Data S1. Materials & Methods.